Genome-wide association study identified BnaPAP17 genes involved in exogenous ATP utilization and regulating phosphorous content in Brassica napus

Article

Accepted Version

Li, H., Liu, H., Wang, C., Zeng, Y., Kant, S., Wang, X., Hammond, J. P. ORCID: https://orcid.org/0000-0002-6241-3551, Ding, G., Cai, H., Wang, S., Xu, F., Zhang, Y. and Shi, L. ORCID: https://orcid.org/0000-0002-5312-8521 (2024)
Genome-wide association study identified BnaPAP17 genes involved in exogenous ATP utilization and regulating phosphorous content in Brassica napus. Plant Cell Reports, 43. 296. ISSN 1432-203X doi: 10.1007/s00299-024-03373-x
Available at https://centaur.reading.ac.uk/120365/

Title: Genome-wide association study identified *BnaPAP17* genes involved in exogenous ATP utilization and regulating phosphorous content in *Brassica napus*

Hao Li[1,2], Haijiang Liu[3], Chuang Wang[2], Yang Zeng[1,2], Surya Kant[4], Xiaohua Wang[5], John P. Hammond[6], Guangda Ding[2], Hongmei Cai[2], Sheliang Wang[2], Fangsen Xu[1,2], Ying Zhang[7*] and Lei Shi[1,2*]

Addresses:

1 National Key Laboratory of Crop Genetic Improvement, Huazhong Agricultural University, Wuhan, 430070, China

2 Microelement Research Centre, Key Laboratory of Arable Land Conservation (Middle and Lower Reaches of Yangtze River), Ministry of Agriculture and Rural Affairs, Huazhong Agricultural University, Wuhan, 430070, China

3 College of Agronomy and Biotechnology, Southwest University, Chongqing, 400715, China

4 School of Agriculture, Biomedicine & Environment, La Trobe University, AgriBio, 5 Ring Rd, Bundoora, Vic 3083, Australia

5 College of Agriculture and Forestry Science, Linyi University, Middle of Shuangling Road, Lanshan District, Linyi, 276000, China

6 School of Agriculture, Policy and Development, University of Reading, Reading RG6 6AR, UK

7 Hunan Institute of Agricultural Environment and Ecology, Hunan Academy of Agricultural Sciences, Changsha 410125, Hunan, China

***Correspondence**

Lei Shi, National Key Laboratory of Crop Genetic Improvement, Huazhong Agricultural University, Wuhan, China.

E-mail: leish@mail.hzau.edu.cn

Ying Zhang, Hunan Institute of Agricultural Environment and Ecology, Hunan Academy of Agricultural Sciences, Changsha, China.

E-mail: zhangying@hunaas.cn

Abstract

***Key Message BnaPAP17s* associated with root-secreted APases activity were identified by genome-wide association study, and those were induced by Pi-deficiency. BnaPAP17s were involved in improving exogenous organophosphorus utilization as secreted APases.**

Abstract Deficiency of available phosphorus (P) in soil has become an important limiting factor for yield and quality in oilseed rape (*Brassica napus*). In many soils, organic P (Po) is the main component of the soil P pool. Po must be hydrolyzed to inorganic P (Pi) through acid Phosphatase (APases), and then taken up by plants. However, root-secreted APases (SAP) activity, as a quantitative trait, plays an important role in soil Po utilization; those genetic loci are not clear in *B. napus*. In this study, we performed a genome-wide association study for SAP activity under Pi-deficieny using a panel of 350 accessions of *B. napus* and more than 4.5 million polymorphic single nucleotide polymorphisms (SNPs). Thirty-five significant SNPs associated with SAP activity were identified. *BnaA01.PAP17* (*BnaA01g27810D*) was a candidate gene underlying lead SNP (ChrA01_19576615). We experimentally verified that both *BnaA01.PAP17* and its three homologous genes had similar expression pattern in response to Pi-deficiency. The dynamic changes in *BnaPAP17s* expression level were opposite to those of Pi concentration in both roots and leaves, suggesting their potential utility as Pi marker genes in *B. napus*. Transient expression of BnaPAP17s in tobacco leaves proved that BnaPAP17s were located in the apoplast as secreted APases. The overexpression of *BnaPAP17s* enhanced SAP activity in response to Pi-deficiency and resulting in increased P content in plants when ATP was supplied as the sole P resource. Taken together, these results suggest that *BnaPAP17s* contributed to SAP activity, thus having a function in extracellular Po utilization in *B. napus*.

Keywords: *Brassica napus*, genome-wide association study (GWAS), organic phosphorus (Po), *BnaPAP17*, root-secreted acid phosphatase

Abbreviations: APases, acid Phosphatases; SAP, root-secreted APases; GWAS, genome-wide association study; GLM, general linear model; MLM, mixed linear model; SNP, single nucleotide polymorphism

Introduction

Oilseed rape (*Brassica napus* L., 2n = 38, genome AACC) is an important oil crop used globally for edible oil, feedstock, and biodiesel production (Angelovi˘c et al., 2013). Phosphorus (P) is the second most important macronutrient for plant growth and development, which makes up around 0.2% of a plant's dry weight (Schachtman et al., 1998; Wang et al., 2021). P also is one of the major limiting nutrients for *B. napus* productivity (Zangani et al., 2021). *B. napus* is sensitive to low soil inorganic P (Pi) availability, and its growth is inhibited with the purpling of cotyledons and dark green old leaves at the seedling stage, and with fewer branch numbers and reduced seed yield at the maturity stage (Ding et al., 2012; Shi et al., 2013; Yuan et al., 2016; Duan et al., 2020). However, Pi can form strong ionic interactions with metal cations (e.g., Fe^{3+}, Al^{3+} and Ca^{2+}) presented in the soil, resulting in the formation of unavailable forms (Chen and Liu, 2016). Pi concentration in most soil solutions ranges between 0.5 and 10 μM, which is often inadequate to meet plant normal growth requirements (Poirier et al., 2022). Organic P (Po) is relatively abundant and around 35-65% of total P in soil, sometimes even as high as 90% in organically managed agricultural soils (Shen et al., 2011; Zhang et al., 2024). However, Po must be hydrolyzed to release Pi by phosphatase, and then taken up by plants; the root-secreted APases (SAP) is involved in this process (Bhadouria and Giri, 2022; Wang and Liu, 2018).

In response to P-deficiency, plants have developed two main strategies to improve P acquisition efficiency (Aslam et al., 2022; Dissanayaka et al., 2021). One strategy is to enhance Pi uptake by exploiting a greater volume of soil through changing root system architecture (Han et al., 2022; Liu, 2021, Poirier et al., 2022). Another strategy is to increase the mobilization of both Po and Pi components from the soil by increasing the release of root exudates into the rhizosphere, including hydrolytic enzymes (e.g., APases, RNase and phytase), carboxylates and protons/hydroxides (Wang et al., 2019; Poirier et al., 2022). Among these strategies, SAP is generally considered to play a key role in mobilizing Po in soils, and thus contribute to the improvement of P acquisition efficiency in plants (Bhadouria and Giri, 2021).

Low P tolerance root traits are quantitative traits controlled by multiple genes (Xu et al., 2023; Zhang et al., 2014). Traditional strategies for studying low P tolerance traits include linkage analysis and genome-wide association study (GWAS) (Qiu et al., 2014; Xu et al., 2023; Xu et al., 2024; Upadhyay et al., 2022; Yang et al., 2010; Zhang et al., 2014). For instance, based on linkage analysis, a total of 62 significant quantitative trait loci (QTL) for RSA, total dry weight, and plant P uptake under high and low P conditions were detected in *B. napus* (Yang et al., 2010); a total of six QTLs for root APases activity and 12 QTLs for APases activity of rhizosphere soil were detected in maize (*Zea mays*) (Qiu et al., 2014). A total of 285 single nucleotide polymorphisms (SNPs) associated with RSA traits were identified by GWAS with 404 accessions of *B. napus* (Wang et al., 2017), and then the glycine-rich protein gene *BnGRP1* was identified as a candidate gene associated with RSA traits under low P conditions (Xu et al., 2023). The accessions with haplotype *BnGRP1Hap1* in the panel demonstrate the longest root length and greatest root weight and overexpression *BnGRP1Hap1* significantly increased the root growth and P uptake in *B. napus* (Xu et al., 2023). In addition, *BnaA05.PAP17* associated with RSA traits was also identified under low P conditions and overexpression of *BnA05.PAP17Hap3* improved the shoot and root growth in *B. napus* (Xu et al., 2024). In maize, total of 34 SNPs were identified for RSA traits by GWAS, and a total of five potential candidate genes in the confidence interval of the above SNPs have been identified (Wang et al., 2019). In soybean (*Glycine max*), combining linkage analysis, GWAS and candidate-gene association analysis for root intracellular APases activity and P content, the *GmACP1* was identified (Zhang et al., 2014). Overexpression of *GmACP1* increased SAP activity and P content

(Zhang et al., 2014). Although previous studies have identified several significant markers associated with root traits, the markers associated with SAP activity remain unclear.

The increase of the SAP activity is a common response to low soil P availability in most crops, such as *B. napus*, wheat (*Triticum aestivum*), rice (*Oryza sative*), soybean, common bean (*Phaseolus vulgaris*) and maize (Bhadouria et al., 2023; Ciereszko et al., 2011; Du et al., 2022; Duan et al., 2020; Li et al., 2024; Liang et al., 2010; Wu et al., 2018; Yu et al., 2019). Acid phosphatases (APases, E.C. 3.1.3.2) have optimal activity below pH 7.0 and can catalyze the hydrolysis of a broad array of Po to release Pi (Bhadouria and Giri, 2022; Wang and Liu, 2018). The Pi released from Po by SAP in the rhizosphere was closely related to the efficiency of P acquisition in crops (Bhadouria and Giri, 2022; Wang and Liu, 2018). SAP activity of P-efficient genotypes was significantly higher than that of P-inefficient genotypes in *B. napus* (Zhang et al 2010), soybean (Zhang et al., 2020; Zhou et al., 2016) and maize (Yu et al., 2019).

Purple acid phosphatase (PAP), with a binuclear metal centre binding either Fe (III)-Zn (II) or Fe (III)-Mn (II) ions and comprising five conserved motif blocks (DXG/GDXXY/GNH(D/E)/VXXH/GHXH), are a kind of important acid phosphatase and have been reported to promote the utilization of exogenous Po in plants (Bhadouria and Giri, 2022; Wang and Liu, 2018). Overexpression of *OsPAP10a*, *OsPAP10c*, *OsPAP26* and *OsPAP21b* lines in rice and overexpression of *GmPAP7a* and *GmPAP7b* in soybean significantly increased the SAP activity and improved the utilization of exogenous ATP (Deng et al., 2020; Gao et al., 2017; Mehra et al., 2017; Tian et al., 2012; Zhu et al., 2020). In addition, overexpression of *GmPAP1-Like* in soybean had a higher ability to utilize exogenous dNTP than wild-type (Wu et al., 2018). In common bean, overexpression of *PvPAP3* and *PvPAP1* helped plants hydrolyze the externally supplied ATP and dNTP (Liang et al., 2010; Liang et al., 2012). In stylo (*Stylosanthes guianensis*), the overexpression lines of *SgPAP7*, *SgPAP10* and *SgPAP26* could use dNTPs as P source (Liu et al., 2016). Recently, 82 PAPs were identified in *B. napus* and overexpression of *BnaA09.PAP10* and *BnaC09.PAP10* in *Arabidopsis* significantly improved the utilization efficiency of exogenous ATP (Zhang et al., 2024).

In this study, the SAP activity of an association panel of 350 accessions of *B. napus* was investigated under Pi-deficient condition. The genetic control of SAP activity was performed using more than 4.5 million SNPs by GWAS. A total of 35 significant SNPs related to SAP activity of *B. napus* were identified, and *BnaA01.PAP17* was identified as a candidate gene associated with SAP activity under Pi-deficient condition. The haplotype *BnaA01.PAP17Hap1* (TACGATCT) with high SAP activity was revealed. Further, four *BnaPAP17s* family genes were identified with high similarity of amino acid in *B. napus*. Overexpression of *BnaPAP17s* increased SAP activity and Po utilization efficiency in *B. napus*. Overall, these results increase our understanding of the function and the genetic variation of *BnaPAP17s*, which will be helpful for the breeding of *B. napus* with higher Po utilization efficiency.

Materials and methods

Plant materials and growth conditions

In this study, firstly, the *B. napus* accessions 'Y127' seeds were washed three times with deionized water and then placed at 4℃ for overnight soaking. The imbibed seeds were germinated on a piece of gauze moistened with deionized water for six days and then transferred to the Hoagland nutrient solution (Hoagland and Arnon, 1950) with 500 μM (+P) or 0 μM (-P) KH_2PO_4 for 0, 1, 3, 5, 7 and 10 days (The monitoring time points refer to Zhang et al. 2010). After that, the plants were used to detect the dynamic change of shoot and root fresh weight, root-secreted APases (SAP) activity and root-intracellular APases (IAP) activity. The results indicated that the SAP activity of 'Y127' was significantly increased by P

deficiency and reached the highest on the 5th day (Fig. 1C). Secondly, an association panel of 350 accessions of *B. napus* with diverse genetic backgrounds, including 303 semi-winter, 41 spring, 4 winter and 2 unknown types collected worldwide was used to investigate the SAP activity under both +P and -P conditions (Table S1). Seeds were germinated with deionized water for six days and then transferred to Hoagland nutrient solution (Hoagland and Arnon, 1950) with 500 μM (+P) or 0 μM (-P) KH_2PO_4 for five days. Then, the plant was used for measurement of the SAP activity for GWAS. All the plants were cultivated in the greenhouse with a 16 h / 8 h (light/dark) at 22℃. Three biological replicates were used for each sample. All the nutrient solutions were renewed every 5 days. The pH of the nutrient solution was adjusted with 1 M HCl or NaOH to 5.6.

Measurement of root APases activity

For measurement of SAP activity, the plant roots were rinsed in distilled water, and subsequently immersed into 5 mL culture medium (pH 5.5) containing 5 mM p-NPP as the substrate. After 30 min at 35℃, the reaction was stopped with 1 M NaOH and the absorbance was determined at 410 nm using a microplate assay (Spark, Tecan, Switzerland). SAP activity was quantified as μmol pNP min^{-1} g^{-1} root fresh weight (Li et al., 2024).

Total protein was extracted from plant roots as described by Lu et al. (2016). Briefly, approximately 0.1 g plant roots were homogenized in frozen extraction buffer and then centrifuged at 12000 rpm at 4°C for 20 min to obtain total protein. The protein content was quantified using the Bradford Protein Quantification Kit (Vazyme, Nanjing, China). For measurement of IAP activity, add 1 μg total proteins to 0.6 mL 50 mM sodium acetate buffer at pH5.5 containing 10 mM pNPP. The reactions were incubated at 35ºC for 30 min and were stopped with 1.2 mL 1 M NaOH and the absorbance was determined at 410 nm using a microplate assay (Spark, Tecan, Switzerland). The IAP activity was expressed as μmol pNP min^{-1} mg^{-1} protein (Lu et al., 2016).

GWAS for root-secreted APases traits

In a previous study, more than 10 million SNPs across this association panel of *B. napus* were identified (Tang et al., 2021). In this study, the population genetic structure was estimated based on the polymorphic SNPs of 350 accessions of *B. napus* through Admixture 1.3.0 software. The Tassel 5.0 software was used for the analysis of the relative kinship matrix (Bradbury et al., 2007). The PopLDdecay3.4.0 software was used to calculate the linkage disequilibrium decay (LD decay) (Zhang et al., 2019). The general linear model (GLM) and mixed linear model (MLM) of TASSEL 5.0 software were used to determine the association between SNP markers and SAP activity (Bradbury et al., 2007). The Quantile-Quantile (QQ) plot and the Manhattan plot were drawn by the R package 'CMplot' in R (version 4.2.1). The threshold for the significance of associations between SNPs and SAP activity was used as $P < 1.71e\text{-}6$ and $P < 1e\text{-}5$.

Identification of candidate genes and haplotype analysis

To identify candidate genes for SAP activity, all genes located in the 200 kb up-/downstream of the candidate lead SNP were selected, and the P-starvation induction (PSI) gene was predicted to be a candidate gene combined with the transcriptome data of *B. napus* roots under +P (500 μM KH_2PO_4) and -P (0 μM KH_2PO_4) conditions. Based on the SNPs detected by resequencing and comparative sequencing, the haplotypes of candidate genes were analysed. HaploView.4.2 software was used to conduct haplotype analysis (Barrett et al., 2005). Haplotypes containing at least 10 accessions of *B. napus* of the panel were used for further comparative analysis, and a Student's *t*-test was used to compare the differences in SAP activity among the haplotypes.

Quantitative real-time PCR (qRT-PCR)

Total RNA was isolated using an Eastep® Super Total RNA Extraction Kit (Promega, Beijing, China) following the manufacturer's instructions, then cDNA was synthesized using HiFiScript gDNA Removal cDNA Synthesis Kit (CWBIO, Shanghai, China) following the manufacturer's instructions. qRT-PCR assays were performed with the Hieff® qPCR SYBR Green Master Mix (Yeasen, Shanghai, China), using an RT-PCR detection system in Bio-Rad's ICYCleriQS fluorescent quantitative PCR instrument. *BnaEF1α* gene was used as an internal control to normalize samples, and relative gene expression levels were measured using the $2^{-\Delta\Delta CT}$ method. Four biological replicates were used for each sample, the value of each biological replicate was the mean of those two technical replicates.

Vector construction and plant transformation

For the *BnaPAP17s* overexpression construct, the full-length coding sequence of each *BnaPAP17s* gene was amplified from *B. napus* accession 'Y127' by PCR and then cloned into the PBI121 vector by using the 2X MultiF Seamless Assembly Mix (ABclonal, Wuhan, China). To generate the *Pro*$_{BnaA01.PAP17}$*::GUS* construct, the 2036 bp promoter sequence of the *BnaA01.PAP17* was amplified by PCR from genomic DNA. The amplified fragment was cloned into the DX2181b vector by using the 2X MultiF Seamless Assembly Mix (ABclonal, Wuhan, China). Transformation of *B. napus* was performed using the hypocotyl of *B. napus* for Agrobacterium infiltration as reported by Dai et al. (2020).

GUS histochemical analysis

GUS histochemical staining was performed using a GUS staining kit (Coolaber, Beijing, China). The *Pro*$_{BnaA01.PAP17}$*::GUS* transgenic plants in nutrient solution with 500 μM KH_2PO_4 for four days, and then transferred to +P (500 μM KH_2PO_4) or -P (500 μM KH_2PO_4) nutrient solution for 15 days. Plant tissues were submerged in GUS staining solution and vacuum infiltrated for 30 min, and then the tissues were incubated at 37ºC for 3 h. After staining, the tissues were washed with 75% ethanol to remove chlorophyll and imaged.

Protein subcellular localization analysis

The coding sequences of each *BnaPAP17s* without a stop codon were separately amplified from 'Y127' by PCR with the primers shown in Table S6 and then cloned into the p35s-GFP vector to generate *35S::BnaPAP17s::GFP* fusion constructs by using the 2X MultiF Seamless Assembly Mix (ABclonal, Wuhan, China). The construct's fusion with GFP and the plasma membrane marker *AtPIP2A-mCherry* were co-transformed into tobacco epidermal cells as described previously (Liu et al., 2016). The fluorescence signals of GFP and mCherry were detected by laser confocal fluorescence microscopy (STELLARIS, Leica, Germany) at 488 nm and 568 nm, respectively.

Tissue Pi concentration and total P content

The Pi concentration was measured using the methods referred to Irving and McLaughlin (2008) and Lu et al. (2016). Briefly, 25 mg fresh tissues were homogenized with 25 μl 5 M H_2SO_4, and then add 1.5 ml distilled water. The supernatant was collected by centrifugation at 12,000 rpm at 4°C. Subsequently, the diluted supernatant was mixed with malachite green reagent (19.4 mM H_3BO_3, 27.64 mM $(NH_4)_6MO_7O_{24}{\cdot}4H_2O$, 2.38 M H_2SO_4, 627.5 μM malachite green and 0.1% polyvinyl alcohol), after 30 min, the absorbance of the reactant was measured at 650 nm wavelength by a microplate assay (Spark, Tecan, Switzerland). The determination of total P content referred to Chen et al. (2007) and Li et al. (2024).

Results

Dynamic changes of *B. napus* biomass and root APases activity under Pi starvation

To investigate the effects of Pi-deficiency on *B. napus* growth and root APases activity, the fresh weight (FW) of shoot and root, root-secreted APases (SAP) and root-intracellular APases (IAP) activity

were determined on 0, 1, 3, 5, 7 and 10 d in *B. napus* under +P and -P conditions. Although the shoot fresh weight (SFW) increased with time during the experimental period under both +P and -P conditions, SFW were significantly higher under +P condition than that under -P condition from 1 d to 10 d (Fig. 1A). SFW of *B. napus* plants decreased by 28.7% on 5 d and 54.9% on 10 d under -P condition compared to +P condition ($P < 0.001$; Fig. 1A). The change of root fresh weight (RFW) with time was very similar to SFW under two contrasting Pi supplies (Fig. 1A, B). However, there were no significant differences in RFW between +P and -P from 1 d to 5 d. The RFW were 29.1% ($P < 0.01$) and 51.1% ($P < 0.001$) higher under -P compared to +P on 7 d and 10 d, respectively (Fig. 1B).

The SAP activity under +P condition did not exhibit a significant change with time, however under -P continually increased from 0 d to 5 d, and then slightly decreased from 7 d to 10 d (Fig. 1C). The SAP activity under -P was significantly higher than under +P during the period from 1 d to 10 d ($P < 0.05$ to 0.001), it reached the highest under -P on 5th d, which was 97% higher than +P (Fig. 1C). Unlike the changes of SAP activity with time, the IAP under +P and -P both decreased from 0 d to 3 d, and then the IAP under -P increased from 3 d to 10 d, and that under +P increased from 3 d to 5 d, and no significant change from 5 d to 10 d (Fig. 1D). There was no significant difference in IAP between +P and -P from 0 d to 7 d, however the IAP under -P was 89% higher than that under -P at 10th d ($P < 0.01$; Fig. 1D). These results indicated that SAP activity had a quick response to Pi starvation than root biomass and IAP activity, which might play an important role in regulating the Pi starvation of *B. napus*.

Phenotypic variation for root-secreted APases activity of an association panel *B. napus*

To identify genotypic differences in the SAP activity of *B. napus*, an association panel of 350 accessions of *B. napus* was used in this study (Table S1). Significant phenotypic variations in SAP activity were observed under both +P (ranged from 0.55 to 2.24, 4.1-fold variation) and -P (ranged from 1.03 to 3.79, 3.7-fold variation), and the coefficient of variation (CV) were 30.8% and 26.2%, respectively (Fig. S1A, B; Table S1). Moreover, the average SAP activity of the *B. napus* panel under -P was higher than that under +P (Fig. S1C). The SAP activity showed an approximately normal distribution among the association panel of *B. napus* under both +P and -P conditions (Fig. S1A, B).

GWAS of root-secreted APases activity in *B. napus*

A total of 4.5 million SNP markers were identified for this association panel of *B. napus.* There was a minimum CV error at K = 4, showing that these accessions in the population can be divided into four subgenomes (Fig. 2A, B). The pairwise relative relationship of most genotypes was less than 0.1, indicating that the 350 accessions of *B. napus* had a weak relationship (Fig. 2C). Based on the cutoff for squared correlations of allele frequencies (r^2) at 0.1, LD decay distance of this natural population was 179 kb (Fig. 2D). These results showed that the genetic distance of the majority of the accessions in the association panel was large enough for the GWAS analysis.

GLM and MLM were used to control the false positives of the genotype-phenotype. Based on a *P-value* < 1.71e-6, a total of 12 and 35 significant SNPs associated with SAP activity of *B. napus* were identified on the 7 and 10 chromosomes by GLM, explaining the range of 7.1 to 9.9% and 6.7 to 10.1 % of phenotypic variation under +P and -P conditions, respectively (Fig. 3A; Fig. S2A; Table S2). Moreover, MLM analysis identified two and three significant SNPs associated with SAP activity of *B. napus* at *P-value* < 1.71e-6 under +P and -P conditions, respectively; 14 and 23 significant SNPs associated with SAP activity of *B. napus* at *P-value* < 1e-5, under +P and -P conditions, respectively (Fig. 3B; Fig. S2B; Table S3). The two highly significant lead SNPs (ChrA01_19576615, ChrC03_3531206) on the A01 and C03 chromosomes explained 10.1% and 9.5% of the phenotypic variation in SAP activity under -P by GLM analysis, respectively (Fig. 3A; Table S2). These SNPs were also significantly associated with SAP

activity at P-value < 1e-5 by MLM (Fig. 3B; Table S3).

The identification of *BnaA01.PAP17*

In this study, the LD decay was 179 kb for this association panel (Fig. 2D). Based on the LD decay, 200 kb up/downstream of the significant SNPs were selected to identify candidate genes. There were 57 genes in the LD decay confidence intervals of both ChrA01_19576615 and ChrC03_3531206, respectively (Table S4). *BnaA01g27810* (*BnaA01.PAP17*) and *BnaC03g07130D* (*BnaC03.RGP2*) within the LD decay of ChrA01_19576615 and ChrC03_3531206, respectively were significantly induced by Pi-deficiency (Fig. 4A-C; Table S4). The expression levels of them under -P were 259 and 2.4-fold higher than that of them under +P, respectively. Among them, *BnaA01.PAP17* encoded purple acid phosphatase and *BnaC03.RGP2* encoded a reversibly glycosylated polypeptide (Table S4). Therefore, we speculated that *BnaA01.PAP17* may be one of the candidate gene associated with SAP activity in *B. napus*.

BnaA01.PAP17 was the homologous gene of *Arabidopsis AtPAP17* (Table S4). To further understand the intragenic variation affecting the phenotypic values and identify the favourable haplotypes, 15 SNPs are located in the promoter and genome sequence of *BnaA01.PAP17* were detected and nine of them significantly associated with SAP activity were detected by candidate gene association analysis at *P-value* < 0.01 (Fig. 4D; Table S5). Among the nine significant SNPs, five were located in the promoter, three in the exon, and one in the intron region (Fig. 4D). Additionally, eight of the nine SNPs formed an LD block in *BnaA01.PAP17* sequence, which was classified into two major haplotypes, *BnaA01.PAP17Hap1* (TACGATCT) and *BnaA01.PAP17Hap2* (AGTAGATC) (Fig. 4D, E). The two haplotypes include 80 and 95 accessions, respectively (Fig. 4E). The *BnaA01.PAP17Hap1* accessions possessed a significantly higher mean SAP activity than the *BnaA01.PAP17Hap2* accessions (Fig. 4F).

***BnaPAP17s* were secreted purple acid phosphatase protein family genes**

Four members of the BnaPAP17s family were identified on chromosomes A01, A05, C01 and C05 in *B. napus*, with higher sequence similarity (at least 91%) (Fig. S3A, B). Among them, BnaA01.PAP17 and BnaC01.PAP17 both contained 333 amino acids, and the amino acid similarity between them was 99% (Fig. S3A, B); BnaA05.PAP17 and BnaC05.PAP17 both contained 337 amino acids, and the amino acid similarity between them was 98% (Fig. S3A, B). BnaPAP17s had a metallophos domain with five conserved motifs predicted by the SMART (http://smart.embl-heidelberg.de) tool, which was a characteristic property of the PAP protein (Fig. S3A). A phylogenetic tree was constructed with the protein sequence of PAPs in some species and BnaPAP17s in *B. napus* using MEGA-X software. These PAPs were clustered into three major groups, and BnaPAP17s were clustered along with AtPAP17 and other low-molecular-weight PAPs in group III (Fig. S3C).

To determine the subcellular localization of BnaPAP17s, the green fluorescent protein (GFP) was fused with each member of the BnaPAP17s family, respectively. All BnaPAP17s and GFP fusion proteins showed co-localized with plasma membrane (PM) markers under control conditions (no plasmolysis treatment) in tobacco leaves (Fig. 5). However, after plasmolysis of tobacco leaves, all BnaPAP17s and GFP fusion proteins showed a blocky green fluorescent filled in apoplast between the two PM (Fig. 5). These results suggested that BnaPAP17s were secreted PAP proteins located in apoplast.

***BnaPAP17s* are involved in exogenous ATP utilization in response to Pi-deficiency**

qRT-PCR was used to determine the expression of *BnaPAP17s* in *B. napus* under Pi-starvation conditions. The results showed that the change in Pi concentration was opposite to the expression level of *BnaPAP17s* (Fig. 6). The concentrations of Pi began to decrease significantly in both leaves and roots of Pi-deficient plants on the 4th day and reached the lowest level on the 10th day (Fig. 6A, B). Resupply of Pi in the nutrient solution rapidly increased the concentrations of Pi in both the roots and leaves (Fig.

6A, B). The decrease in Pi concentration in both leaves and roots was accompanied by a significant increase in the expression of each member of *BnaPAP17s* of Pi-deficient plants on the 4th day, reached the highest level on the 10th day, and rapidly decreased with resupply of Pi in the nutrient solution (Fig. 6C-J). In addition, *Pro$_{BnaA01.PAP17}$::GUS* transgenic plant was used to determine the tissue-specific expression of *BnaA01.PAP17*. The results showed that *BnaA01.PAP17* was induced by Pi-deficiency in both leaves and roots, which were similar to qRT-PCR (Fig. 7).

Two genotypes with high SAP activity (383, 385) and two genotypes with low SAP activity (124, 286) were selected from the association panel of 350 accessions of *B. napus* to measure gene expression of *BnaPAP17s* by qRT-PCR under +P and -P conditions. The SAP activity was increased in response to Pi-deficient stress among four genotypes (Fig. 8A). Moreover, compared with +P condition, the expression of *BnaPAP17s* among four genotypes was all strongly increased under -P condition (Fig. 8B-E). The expression level of *BnaPAP17s* was lower in the roots of high SAP activity genotypes than that of low SAP activity genotypes under +P condition (Fig. 8B-E). However, the expression level of *BnaPAP17s* in the roots of high SAP activity genotypes was higher than that of low SAP activity genotypes (especially 383) under -P condition (Fig. 8B-E). These results provided further evidence that the four *BnaPAP17s* were closely associated with SAP activity in response to low Pi stress.

To further demonstrate the effect of *BnaPAP17s* on SAP activity in response to Pi-deficiency in *B. napus*, we constructed the overexpression transgenic (OE) plants of each member of the *BnaPAP17s* family in *B. napus*. The expression of all the *BnPAP17s* was significantly higher in four different OE lines than in wild-type (WT) (Fig. 9A). Furthermore, we assessed the SAP activity in OE lines under +P and -P conditions. The OE lines had higher SAP activity than WT under -P, condition but there was no or a slight difference in SAP activity between OE and WT lines under +P condition (Fig. 9B, C). In addition, there was not significant difference in biomass between OE and WT lines among the three P treatments (Fig. S4). Although there was no difference in P content between OE and WT lines under +P and -P conditions, the OE lines had significantly increased P content compared with WT lines when ATP was supplied as the sole P resource (Fig. 9D). These results further demonstrated that *BnaPAP17s* were closely related to SAP activity in response to Pi-deficiency and were involved in the process of exogenous Po utilization.

Discussion

Root-secreted APases activity in response to Pi deficiency

In plants, it is common to change RSA traits and increase SAP activity in response to Pi deficiency (Liu, 2021; Poirier et al., 2022; Wang et al., 2019). SAP is generally thought to increase P availability by hydrolyzing Po, and RSA traits are changed to improve P uptake through larger exploration of the soil volume (Liu, 2021; Poirier et al., 2022; Wang et al., 2019). Our previous study also reported that the root biomass and SAP activity increased in response to Pi-deficiency in *B. napus* (Duan et al., 2020; Li et al., 2024). In this study, although root biomass, SAP activity and IAP activity were all increased under Pi-deficient conditions, the SAP activity responded more quickly than RFW and IAP activity to Pi-deficiency. It is indicated that SAP also plays an important role in the adaptability of *B. napus* to Pi deficiency. Among them, the SAP activity, RFW and IAP activity of *B. napus* began to increase on 1 d, 7 d and 10 days when the plants suffered Pi-deficiency, respectively (Fig. 1B-D). Unlike *B. napus*, in soybean, the SAP and IAP activity began to increase on 1 d in response to Pi-deficiency, and the SAP activity was lower than IAP activity (Zhu et al., 2020). The IAP activity of the suspension cells of the tomato (*Lycopersicon esculentum*) under Pi-deficiency began to increase on 6 d, reached to the highest on 11 d, but decreased to the same activity as Pi-sufficient conditions on 14 d (Bozzo et al., 2006).

However, the SAP activity under Pi-deficiency began to increase on 8 d and increased linearly with the time of culture (Bozzo et al., 2006). These indicated that the response time of SAP and its activity under Pi-deficiency differs in different species.

Identification of SNP markers and candidate gene controlling SAP activity in *B. napus*

In plants, low P tolerance-related traits are complex and controlled by multiple genes (Xu et al., 2023; Zhang et al., 2014). Several genes that respond to low-P stress have been identified in crops by GWAS and linkage analysis. For instance, *GmSPX-RING1*, *GmPHF1* and *GmEIL4* involved in enhancing low-P tolerance were identified in soybean (Du et al., 2020; Guo et al., 2022; Yang et al., 2023). *OsACP2* and *OsAAD* enhanced phosphorus use efficiency in rice (Liu et al., 2024; Yan et al., 2023), *BnGRP1* and *BnaA05.PAP17* were associated with RSA, and enhanced low-P tolerance in *B. napus* (Xu et al., 2023, Xu et al., 2024). The discovery and application of the genetic loci and candidate genes controlling low-P tolerance-related traits have become increasingly important in plant breeding. However, the identification of SNP markers and candidate genes associated with APases activity is often overlooked. A major QTL *qPE8* associated with IAP activity and plant P content was identified through GWAS and linkage analysis (Zhang et al., 2014).

In this study, genetic variations related to SAP activity under Pi-deficient stress were detected by GWAS using 4.5 million SNP markers in a natural population with 350 accessions of *B. napus* (Table S1). A total of 35 SNPs associated with SAP activity were identified, and among them, the lead SNP ChrA01_19576615 and ChrC03_3531206 were detected by GLM and MLM (Fig. 3; Tables S2 and S3). *BnaA01.PAP17* and *BnaC03.RGP2* were identified in the confidence interval of ChrA01_19576615 and ChrC03_3531206, respectively, they were significantly induced by Pi-deficient in *B. napus* roots. The up-regulated expression level of *BnaA01.PAP17* was much higher than that of *BnaC03.RGP2* under P deficiency (Table S4). Therefore, the *BnaA01.PAP17* was identified to be the candidate gene associated with SAP activity in response to P-deficient stress.

The discovery of the superior haplotype of candidate genes can contribute to breed elite crop varieties (Gao et al., 2019; Wang et al., 2021; Zhang et al., 2023). In this study, 15 SNPs were detected in the 2 kb promoter and coding sequence of *BnaA01.PAP17*, and eight SNPs among them associated with SAP activity formed an LD block (Fig. 4D). Based on these SNPs, two typical haplotypes containing 80 and 95 accessions were identified, respectively (Fig. 4E). The SAP activity of *BnaA01.PAP17Hap1* was significantly higher than *BnaA01.PAP17Hap2* under Pi-deficient conditions (Fig. 4F). *BnaA01.PAP17Hap1* is a superior haplotype and may be used to breed P-efficient *B. napus* varieties in the future, though might need further study. Recently, five sequence variations of *SbAT1* were identified with higher relative survival rates under alkali treatment in sorghum (*Sorghum bicolor*) with Hap1 showing much higher survival rates than Hap2 (Zhang et al., 2023). Further, the *SbAT1* homologs in rice, maize and millet (*Setaria italica*) had similar roles, and genetically engineered crops with knockouts of *AT1* homologs or use of natural nonfunctional alleles could greatly improve crop yield in sodic lands (Zhang et al., 2023). Additionally, the sequence of *TaPHT1;9-4B* displays haplotype variation, and Hap3 of *TaPHT1;9-4B* showed higher growth performance and P content than other haplotypes in wheat genotypes (Wang et al., 2021).

BnaPAP17s associated with SAP activity were involved in exogenous ATP utilization

It has been reported that Pi starvation induces SAP activity, which degrades Po into Pi for plant uptake (Bhadouria and Giri, 2021, Wang and Liu, 2018). PAPs are a distinct group of APases, that are widely studied for their roles in plant acclimation to Pi deficiency, and most *PAPs* are reported to be induced transcriptionally in response to Pi deficiency (Bhadouria and Giri, 2021). For instance, 10, 12,

24, 20 and 11 PAPs were induced by Pi-deficient in rice, chickpea (*Cicer arietinum*), soybean, tomato (*Solanum lycopersicum*) and maize, respectively (Bhadouria et al., 2017; Gonzalez-Munoz et al., 2015; Li et al., 2012; Srivastava et al., 2020; Zhang et al., 2011). In this study, four members of *BnaPAP17s* with high sequence similarity were identified in *B. napus* (Fig. S3A, B). Similar expression profiles were observed among the *BnaPAP17* gene family in response to Pi deficiency. The expression of *BnaPAP17s* in both roots and leaves was induced by Pi-deficiency. The expression of *BnaPAP17s* increased continuously with the decrease of Pi concentration in Pi-deficient plants and decreased rapidly with the increase of P in both roots and leaves by resupply of Pi (Fig. 6). These suggested that *BnaPAP17s* could be used as Pi marker genes in *B. napus*.

In this study, we found that the genotypes with high SAP activity had higher expression of *BnaPAP17s* than genotypes with low SAP activity under Pi-deficient conditions (Fig. 8). This suggested that the expression of *BnaPAP17s* could be related to SAP activity in response to Pi-deficiency. *AtPAP10, AtPAP12* and *AtPAP26* are the main secreted APases genes, and overexpression of these significantly increased the SAP activity and promoted the utilization of exogenous Po (i.e., ADP and Fru-6-P) in *Arabidopsis* (Wang et al., 2014). Additionally, overexpression of *OsPAP10a*, *OsPAP10c* and *OsPAP26* also increased the SAP activity and promoted the utilization of exogenous ATP in rice (Deng et al., 2020; Gao et al., 2017; Tian et al., 2012). In this study, overexpression of *BnaPAP17s* significantly increased SAP activity under Pi-deficiency. Although the overexpression of *BnaPAP17s* had no effect on total P content under Pi-sufficient and Pi-deficient conditions, it significantly increased the total P content when ATP was used as a P source (Fig. 9). These results suggested that *BnaPAP17* genes were associated with SAP activity and involved in exogenous ATP utilization in *B. napus*. In addition, there was not significant difference in biomass between OE and WT lines when ATP was supplied as the sole P resource (Fig. S4). This is likely due to the fact that both OE and WT roots secrete APases to hydrolyze ATP and obtain enough Pi for plant growth.

Conclusion

In *B. napus*, the SAP activity responded more quickly to Pi deficiency than IAP activity and root growth. A total of 35 SNPs associated with SAP activity were identified by GWAS in an association panel of 350 accessions of *B. napus* and *BnaA01.PAP17* was identified within the LD decay confidence interval of lead SNP (ChrA01_19576615). The genotypes of *BnaA01.PAP17Hap1* had higher SAP activity than those of *BnaA01.PAP17Hap2*. All the four members of the BnaPAP17s were located in the apoplast and were secreted APases. Overexpression of *BnaPAP17s* significantly enhanced exogenous ATP utilization by increasing SAP activity. *BnaPAP17s* and the favorable haplotype of *BnaA01.PAP17* could be important candidate gene for the breeding *B. napus* with high Po-efficient utilization.

Author contribution statement

SL and ZY designed research and critically review and editing. **LH** performed research, collected phenotypes, performed data analysis and wrote draft manuscript. **LHJ, WC and ZY** performed data analysis and performed draft review. **SK, WXH and JPH** performed draft review. **DGD,CHM, WSL and XFS** performed data analysis. All authors have read and approved the final version of manuscript.

Declarations

Conflict of interest The authors declare that they have no known competing financial interests or personal relationships that could have appeared to influence the work reported in this paper.

Data Availability

The datasets generated during and/or analysed during the current study are available from the corresponding author on reasonable request.

Funding

This work was supported by the National Key Research and Development Program of China (Grants No. 2023YFD1700204), Agricultural Science and Technology Innovation Funds Project of Hunan Province (Grants No. 2023CX105) and National Nature Science Foundation of China (Grants No. 32172662).

Supporting information

Supplementary data associated with this article can be found in the online version

References

Angeloviˇc M, Tkaˇc Z, Angeloviˇc M (2013) Oilseed rape as feedstock for biodiesel production in relation to the environment and human health. Potravinarstvo Slovak Journal of Food Sciences. 7, 101-106. https://doi.org/10.5219/278

Aslam MM, Karanja JK, Dodd IC, Waseem M, Weifeng X (2022) Rhizosheath: An adaptive root trait to improve plant tolerance to phosphorus and water deficits?. Plant Cell Environ 45, 2861-2874. https://doi.org/10.1111/pce.14395

Barrett JC, Fry B, Maller J, Daly MJ (2005) Haploview: analysis and visualization of LD and haplotype maps. Bioinformatics. 21, 263-265. https://doi.org/10.1093/bioinformatics/bth457

Bhadouria J, Giri J (2021) Purple acid phosphatases: roles in phosphate utilization and new emerging functions. Plant Cell Rep. 41, 33-51. https://doi.org/10.1007/s00299-021-02773-7

Bhadouria J, Mehra M, Verma L, Pazhamala LT, Rumi R, Panchal P, Sinha AK, Giri J (2023) Root-expressed rice PAP3b enhances secreted APases activity and helps utilize organic phosphate. Plant Cell Physiol. 64, 501-518. https://doi.org/10.1093/pcp/pcad013

Bhadouria J, Singh AP, Mehra P, Verma L, Srivastawa R, Parida SK, Giri J (2017) Identification of purple acid phosphatases in chickpea and potential roles of CaPAP7 in seed phytate accumulation. Sci. Rep. 7, 11012. https://doi.org/10.1038/s41598-017-11490-9

Bozzo GG, Dunn EL, Plaxton WC (2006) Differential synthesis of phosphate-starvation inducible purple acid phosphatase isozymes in tomato (*Lycopersicon esculentum*) suspension cells and seedlings. Plant Cell Environ. 29: 303-313. https://doi.org/10.1111/j.1365-3040.2005.01422.x

Bradbury PJ, Zhang ZW, Kroon DE, Casstevens TM, Ramdoss Y, Buckler ES (2007) TASSEL: software for association mapping of complex traits in diverse samples. Bioinformatics. 23, 2633-2635. https://doi.org/10.1093/bioinformatics/btm308

Chen AQ, Hu J, Sun SB, Xu GH (2007) Conservation and divergence of both phosphate- and mycorrhiza-regulated physiological responses and expression patterns of phosphate transporters in solanaceous species. New Phytol 173, 817-831. https://doi.org/10.1111/j.1469-8137.2006.01962.x

Chen ZC, Liao H (2016) Organic acid anions: An effective defensive weapon for plants against aluminium toxicity and phosphorus deficiency in acidic soils. J Genet Genomics. 43, 631-638. https://doi.org/10.1016/j.jgg.2016.11.003

Ciereszko I, Szczygla A, Zebrowska E (2011) Phosphate deficiency affects acid phosphatase activity and growth of two wheat varieties. J Plant Nutr. 34, 815-829. https://doi.org/10.1080/01904167.2011.544351

Dai C, Li YQ, Li L, Du ZL, Lin SL, Tian X, Li SJ, Yang B, Yao W, Wang J, Guo L, Lu SP (2020) An efficient Agrobacterium-mediated transformation method using hypocotyl as explants for *Brassica napus*. Mol. Breed. 40, 96. https://doi.org/10.1007/s11032-020-01174-0

Deng SR, Lu LH, Li JY, Du ZZ, Liu TT, Li WJ, Xu FS, Shi L, Shou HX, Wang C (2020) Purple acid phosphatase 10c encodes a major acid phosphatase that regulates plant growth under phosphate-

deficient conditions in rice. J. Exp. Bot. 71, 4321-4332. https://doi.org/10.1093/jxb/eraa179
Ding GD, Zhao ZK, Liao Y, Hu YF, Shi L, Long Y, Xu FS (2012) Quantitative trait loci for seed yield and yield-related traits, and their responses to reduced phosphorus supply in *Brassica napus*. Ann. Bot. 109, 747-759. https://doi.org/10.1093/aob/mcr323
Dissanayaka DMSB, Ghahremani M, Siebers M, Wasaki J, Plaxton WC (2021) Recent insights into the metabolic adaptations of phosphorus deprived plants. J. Exp. Bot 72, 199-223 https://doi.org/10.1093/jxb/eraa482
Du WK, Ning LH, Liu YS, Zhang SX, Yang YM, Wang Q, Chao SQ, Yang H, Huang F, Cheng H, Yu DY (2020) Identification of loci and candidate gene *GmSPX-RING1* responsible for phosphorus efficiency in soybean via genome-wide association analysis. BMC Genom. 21, 725. https://doi.org/10.1186/s12864-020-07143-3
Du ZZ, Deng SR, Wu ZX, Cai HM, Xu FS, Shi L, Wang SL, Ding GD, Wang C (2022) Characterization of the phosphate response 2-dependent and -independent Pi-starvation response secretome in rice. J. Exp. Bot. 73, 6955-6970. https://doi.org/10.1093/jxb/erac342
Duan XJ, Jin KM, Ding GD, Wang C, Cai HM, Wang SL, White PJ, Xu FS, Shi L (2020) The impact of different morphological and biochemical root traits on phosphorus acquisition and seed yield of *Brassica napus*. Field Crop Res. 258, 107960. https://doi.org/10.1016/j.fcr.2020.107960
Gao WW, Lu LH, Qiu WM, Wang C, Shou HX (2017) OsPAP26 encodes a major purple acid phosphatase and regulates phosphate remobilization in rice. Plant Cell Physiol. 58, 885-892. https://doi.org/10.1093/pcp/pcx041
Gao ZY, Wang YF, Chen G, Zhang AP, Yang SL, Shang LG, Wang DY, Ruan BQ, Liu CL, Jiang HZ et al (2019) The indica nitrate reductase gene *OsNR2* allele enhances rice yield potential and nitrogen use efficiency. Nat. Commun. 10, 5207. https://doi.org/10.1038/s41467-019-13110-8
Gonzalez-Munoz E, Avendano-Vazquez AO, Montes RA, de Folter S, Andres-Hernandez L, Abreu-Goodger C, Sawers RJ (2015) The maize (*Zea mays ssp*. mays var. B73) genome encodes 33 members of the purple acid phosphatase family. Front. Plant Sci. 6: 341. https://doi.org/10.3389/fpls.2015.00341
Guo ZL, Cao HR, Zhao J, Bai S, Peng WT, Li J, Sun LL, Chen LY, Lin ZH, Shi C et al (2022) A natural uORF variant confers phosphorus acquisition diversity in soybean. Nat. Commun. 13, 3796. https://doi.org/10.1038/s41467-022-31555-2
Han Y, White PJ, Cheng LY (2022) Mechanisms for improving phosphorus utilization efficiency in plants. Annals of Botany 129(3): 247-258. https://doi.org/10.1093/aob/mcab145
Hoagland DR, Arnon DI (1950) The water culture method for growing plants without soil. Circular 347, 2nd ed. Berkeley, CA: California Agricultural Experiment Station, University of California.
Irving GCJ, McLaughlin MJ (2008) A rapid and simple field test for phosphorus in Olsen and Bray No. 1 extracts of soil. Commun. Soil Sci. Plant Anal. 21, 2245-2255. https://doi.org/10.1080/00103629009368377
Li CC, Gui SH, Yang T, Walk T, Wang XR, Liao H (2012) Identification of soybean purple acid phosphatase genes and their expression responses to phosphorus availability and symbiosis. Ann. Bot. 109, 275-285. https://doi.org/10.1093/aob/mcr246
Liang CY, Tian J, Lam HM, Lim BL, Yan XL, Liao H (2010) Biochemical and molecular characterization of PvPAP3, a novel purple acid phosphatase isolated from common bean enhancing extracellular ATP utilization. Plant Physiol. 152, 854-865. https://doi.org/10.1104/pp.109.147918
Liang CY, Sun LL, Yao ZF, Liao H, Tian J (2012) Comparative analysis of *PvPAP* gene family and their functions in response to phosphorus deficiency in common bean. PLoS One. 7, e38106.

https://doi.org/10.1371/journal.pone.0038106
Li H, Wang C, Zhang BB, Liu HJ, Hammond JP, Wang XH, Ding GD, Cai HM, Wang SL, Xu FS, Shi L (2024) Trade-offs between root-secreted acid phosphatase and root morphology traits, and their contribution to phosphorus acquisition in *Brassica napus*. Physiol. Plant. 176, e14247. https://doi.org/10.1111/ppl.14247
Liu D (2021) Root developmental responses to phosphorus nutrition. J Integr Plant Biol. 63, 1065-1090. https://doi.org/10.1111/jipb.13090
Liu PD, Xue YB, Chen ZJ, Liu GD, Tian J (2016) Characterization of purple acid phosphatases involved in extracellular dNTP utilization in *Stylosanthes*. J. Exp. Bot. 67, 4141-4154. https://doi.org/10.1093/jxb/erw190
Liu SS, Xu Z, Essemine J, Liu YM, Liu CD, Zhang FX, Iqbal Z, Qu MN (2024) GWAS unravels acid phosphatase ACP2 as a photosynthesis regulator under phosphate starvation condition through modulating serine metabolism in rice. Plant Commun. 19, 100885. https://doi.org/10.1016/j.xplc.2024.100885
Lu LH, Qiu WM, Gao WW, Tyerman SD, Shou HX, Wang C (2016) OsPAP10c, a novel secreted acid phosphatase in rice, plays an important role in the utilization of external organic phosphorus. Plant Cell Environ. 39, 2247-2259. https://doi.org/10.1111/pce.12794
Mehra P, Pandey BK, Giri J (2017) Improvement in phosphate acquisition and utilization by a secretory purple acid phosphatase (OsPAP21b) in rice. Plant Biotechnol. J.15, 1054-1067. https://doi.org/10.1111/pbi.12699
Poirier Y, Jaskolowski A, Clúa J (2022) Phosphate acquisition and metabolism in plants. Curr. Biol. 32, R623-R629. https://doi.org/10.1016/j.cub.2022.03.073
Qiu HB, Liu CX, Yu TT, Mei XP, Wang GQ, Wang JG, Cai YL (2014) Identification of QTL for acid phosphatase activity in root and rhizosphere soil of maize under low phosphorus stress. Euphytica. 197, 133-143. https://doi.org/10.1007/s10681-013-1058-0
Schachtman DP, Reid RJ, Ayling SM (1998) Phosphorus uptake by plants: From soil to cell. Plant Physiol. 116, 447-453. https://doi.org/10.1104/pp.116.2.447
Shen JB, Yuan LX, Zhang JL, Li HG, Bai ZH, Chen XP, Zhang WF, Zhang FS (2011) Phosphorus dynamics: from soil to plant. Plant Physiol. 156, 997-1005. https://doi.org/10.1104/pp.111.175232
Shi TX, Li RY, Zhao ZK, Ding GD, Long Y, Meng JL, Xu FS, Shi L (2013) QTL for yield traits and their association with functional genes in response to phosphorus deficiency in *Brassica napus*. PLoS One. 8, e54559. https://doi.org/10.1371/journal.pone.0054559
Srivastava R, Akash, Parida AP, Chauhan PK, Kumar R (2020) Identification, structure analysis, and transcript profiling of purple acid phosphatases under Pi deficiency in tomato (*Solanum lycopersicum* L.) and its wild relatives. Int. J. Biol. Macromol. 165, 2253-2266. https://doi.org/10.1016/j.ijbiomac.2020.10.080
Tang S, Zhao H, Lu SP, Yu LQ, Zhang GF, Zhang YT, Yang QY, Zhou YM, Wang XM, Ma W, Xie WB, Guo L (2021) Genome- and transcriptome-wide association studies provide insights into the genetic basis of natural variation of seed oil content in *Brassica napus*. Molecular Plant 14: 470-487. https://doi.org/10.1016/j.molp.2020.12.003
Tian JL, Wang C, Zhang Q, He XW, Whelan J, Shou HX (2012) Overexpression of OsPAP10a, A root-associated acid phosphatase, increased extracellular organic phosphorus utilization in rice. J Integr Plant Biol. 54, 631-639. https://doi.org/10.1111/j.1744-7909.2012.01143.x
Upadhyay P, Gupta M, Sra SK, Sharda R, Sharma S, Sardana VK, Akhatar J, Kaur G (2022) Genome-

wide association studies for acid phosphatase activity at varying phosphorous levels in *Brassica juncea* L. Front. Plant Sci. 13, 1056028. https://doi.org/10.3389/fpls.2022.1056028

Wang HM, Wei J, Li PC, Wang YY, Ge ZZ, Qian JY, Fan YY, Ni JR, Xu Y, Yang ZF, Xu CW (2019) Integrating GWAS and gene expression analysis identifies candidate genes for root morphology traits in maize at the seedling stage. Genes-Basel. 10, 773. https://doi.org/10.3390/genes10100773

Wang LS, Liu D (2018) Functions and regulation of phosphate starvation-induced secreted acid phosphatases in higher plants. Plant Sci. 271, 108-116. https://doi.org/10.1016/j.plantsci.2018.03.013

Wang LS, Lu S, Zhang Y, Li Z, Du XQ, Liu D (2014) Comparative genetic analysis of Arabidopsis purple acid phosphatases AtPAP10, AtPAP12, and AtPAP26 provides new insights into their roles in plant adaptation to phosphate deprivation. J Integr Plant Biol. 56: 299-314. https://doi.org/10.1111/jipb.12184

Wang PF, Li GZ, Li GW, Yuan SS, Wang CY, Xie YX, Guo TC, Kang GZ, Wang DW (2021) *TaPHT1;9-4B* and its transcriptional regulator *TaMYB4-7D* contribute to phosphate uptake and plant growth in bread wheat. New Phytol. 231, 1968-198. https://doi.org/10.1111/nph.17534

Wang W, Ding GD, White PJ, Wang XH, Jin KM, Xu FS, Shi L (2019) Mapping and cloning of quantitative trait loci for phosphorus efficiency in crops: opportunities and challenges. Plant Soil. 439, 91-112. https://doi.org/10.1007/s11104-018-3706-6

Wang XH, Chen YL, Thomas CL, Ding GD, Xu P, Shi DX, Grandke F, Jin KM, Cai HM, Xu FS, Shi L (2017) Genetic variants associated with the root system architecture of oilseed rape (*Brassica napus* L.) under contrasting phosphate supply. DNA Res 24: 407-417. https://doi.org/10.1093/dnares/dsx013

Wang Y, Wang F, Lu H, Liu Y, Mao CZ (2021) Phosphate uptake and transport in plants: An elaborate regulatory system. Plant Cell Physiol. 62: 564-572. https://doi.org/10.1093/pcp/pcab011

Wu WW, Lin Y, Liu PD, Chen QQ, Tian J, Liang CY (2018) Association of extracellular dNTP utilization with a GmPAP1-like protein identified in cell wall proteomic analysis of soybean roots. J. Exp. Bot. 69, 603-617. https://doi.org/10.1093/jxb/erx441

Xu P, Li H, Li HY, Zhao G, Dai SJ, Cui XY, Liu ZN, Shi L, Wang XH (2024) Genome-wide and candidate gene association studies identifies *BnPAP17* conferring utilization of organophosphorus in oilseed rape. J. Integr. Agric. 23: 1134-1149. https://doi.org/10.1016/j.jia.2023.05.002

Xu P, Li HY, Xu K, Cui XY, Liu ZN, Wang XH (2023) Genetic variation in *BnGRP1* contributes to low phosphorus tolerance in *Brassica napus*. J. Exp. Bot. 74, 3531-3543. https://doi.org/10.1093/jxb/erad114

Yan M, Feng FJ, Xu XY, Fan PQ, Lou QJ, Chen L, Zhang AN, Luo L, Mei HW (2023) Genome-wide association study identifies a gene conferring high physiological phosphorus use efficiency in rice. Front. Plant Sci. 14, 1153967. https://doi.org/10.3389/fpls.2023.1153967

Yang M, Ding GD, Shi L, Feng J, Xu FS, Meng JL (2010) Quantitative trait loci for root morphology in response to low phosphorus stress in *Brassica napus*. Theor. Appl. Genet. 121, 181-193. https://doi.org/10.1007/s00122-010-1301-1

Yang YM, Wang RY, Wang L, Cui RF, Zhang HY, Che ZJ, Hu DD, Chu SS, Jiao YQ, Yu DY, Zhang D (2023) *GmEIL4* enhances soybean (*Glycine max*) phosphorus efficiency by improving root system development. Plant Cell Environ. 46, 592-606. https://doi.org/10.1111/pce.14497

Yu TT, Liu CX, Lu XF, Bai Y, Zhou L, Cai YL (2019) *ZmAPRG*, an uncharacterized gene, enhances acid phosphatase activity and Pi concentration in maize leaf during phosphate starvation. Theor. Appl. Genet. 132, 1035-1048. https://doi.org/10.1007/s00122-018-3257-5

Yuan P, Ding GD, Cai HM, Jin KM, Broadley MR, Xu FS, Shi L (2016) A novel Brassica-rhizotron

system to unravel the dynamic changes in root system architecture of oilseed rape under phosphorus deficiency. Ann. Bot. 118, 173-184. https://doi.org/10.1093/aob/mcw083

Zangani E, Afsahi K, Shekari F, Mac Sweeney E, Mastinu A (2021) Nitrogen and phosphorus addition to soil improves seed yield, foliar stomatal conductance, and the photosynthetic response of rapeseed (*Brassica napus* L.). Agriculture. 11, 483. https://doi.org/10.3390/agriculture11060483

Zhang C, Dong SS, Xu JY, He WM, Yang TL (2019) PopLDdecay: a fast and effective tool for linkage disequilibrium decay analysis based on variant call format files. Bioinformatics. 35, 1786-1788. https://doi.org/10.1093/bioinformatics/bty875

Zhang D, Song HN, Cheng H, Hao DR, Wang H, Kan GZ, Jin HX, Yu DY (2014) The acid phosphatase-encoding gene *GmACP1* contributes to soybean tolerance to low-phosphorus stress. PLoS Genet. 10, e1004061. https://doi.org/10.1371/journal.pgen.1004061

Zhang H, He XY, Munyaneza V, Zhang GZ, Ye XS, Wang C, Shi L, Wang X, Ding GD (2024) Acid phosphatase involved in phosphate homeostasis in *Brassica napus* and the functional analysis of *BnaPAP10s*. Plant Physiol. Biochem. 208, 108389. https://doi.org/10.1016/j.plaphy.2024.108389

Zhang HW, Huang Y, Ye XS, Xu FS (2010) Analysis of the contribution of acid phosphatase to P efficiency in *Brassica napus* under low phosphorus conditions. Sci. China Life Sci. 53, 709-717. https://doi.org/10.1007/s11427-010-4008-2

Zhang HY, Yang YM, Sun CY, Liu XQ, Lv LL, Hu ZB, Yu DY, Zhang D (2020) Up-regulating *GmETO1* improves phosphorus uptake and use efficiency by promoting root growth in soybean. Plant Cell Environ. 43, 2080-2094. https://doi.org/10.1111/pce.13816

Zhang HL, Yu FF, Xie P, Sun SY, Qiao XH, Tang SY, Chen CX, Yang S, Mei C, Yang DK et al (2023) A Ggamma protein regulates alkaline sensitivity in crops. Science. 379, eade8416. DOI: 10.1126/science.ade8416

Zhang K, Zheng DF, Gu Y, Xu J, Wang MY, Mu B, Wen SJ, Tang T, Rengel Z, Shen JB (2024) Utilizing soil organic phosphorus for sustainable crop production: insights into the rhizosphere. Plant Soil. 498: 57-75. https://doi.org/10.1007/s11104-023-06136-x

Zhang Q, Wang C, Tian J, Li K, Shou HX (2011) Identification of rice purple acid phosphatases related to phosphate starvation signalling. Plant Biol (Stuttg). 13, 7-15. https://doi.org/10.1111/j.1438-8677.2010.00346.x

Zhou T, Du YL, Ahmed S, Liu T, Ren ML, Liu WG, Yang WY (2016) Genotypic differences in phosphorus efficiency and the performance of physiological characteristics in response to low phosphorus stress of soybean in southwest of china. Front. Plant Sci. 7, 1776. https://doi.org/10.3389/fpls.2016.01776

Zhu SN, Chen MH, Liang CY, Xue YB, Lin SL, Tian J (2020) Characterization of purple acid phosphatase family and functional analysis of *GmPAP7a/7b* involved in extracellular ATP utilization in soybean. Front. Plant Sci. 11, 661. https://doi.org/10.3389/fpls.2020.00661

Figure legends

Fig. 1 Dynamic changes in shoot and root fresh weight, root-secreted and -intracellular APases activity in *B. napus*. (A) shoot and (B) root fresh weight. (C) Root-secreted APases activity and (D) root-intracellular APases activity. Seeds of 'Y127' were germinated for six days and then transferred to Pi-sufficient (+P, 500 μM KH_2PO_4) or -deficient (-P, 0 μM KH_2PO_4) nutrient solution for ten days. The data represent the means of six replicates for root and shoot fresh weight, and three replicates for root-secreted and -intracellular APases activity, along with their corresponding standard errors. Asterisks indicate significant differences between the -P and +P treatments by according to Student's *t*-test: $*P < 0.05$; $**P < 0.01$; $***P < 0.001$

Fig. 2 The population structure, relative kinship and LD decay of the *B. napus* association panel. (A) The population structure plot. (B) The cross-validation error value. (C) The pairwise relationship of the *B. napus* association panel. (D) The LD decay plot, squared correlations of allele frequencies (r^2) at 0.1, LD decay distance of this natural population was 179 Kb

Fig. 3 Genome-wide association study for root-secreted APases activity of *B. napus* association panel under Pi-deficient condition. The Manhattan and QQ plot by (A) GLM and (B) MLM. The horizontal dashed line represents the significance threshold with $-\log_{10}(P) = 5.77$ (red) and $-\log_{10}(P) = 5$ (blue)

Fig. 4 The significant SNPs associated with root-secreted APases activity on chromosome A01 and haplotype types of *BnaA01.PAP17* in the *B. napus* association panel. (A) The significant SNP locus on chromosome A01. (B) The expression level of the genes in the confidence interval of ChrA01_19576615 under Pi -sufficient (+P, 500 μM KH_2PO_4) and -deficient (-P, 0 μM KH_2PO_4) conditions. (C) The expression level of *BnaA01.PAP17*. (D) Candidate gene association analysis of *BnaA01.PAP17* with root-secreted APases activity, and the significant SNPs were located in exon (green), intron (grey) and yellow (promoter). (E) The haplotype types of *BnaA01.PAP17*. (F) The difference of root-secreted APases activity between Hap1 and Hap2, Student's *t*-test was used for comparisons between two haplotypes of *B. napus* ($*P < 0.05$)

Fig. 5 Subcellular localization of BnaPAP17s family. GFP protein of (A) BnaA01.PAP17, (B) BnaC01.PAP17, (C) BnaA05.PAP17 and (D) BnaC05.PAP17 before or after plasmolyzing

Fig. 6 Dynamic changes of Pi concentration and expression of *BnaPAP17s* in root and leaf under Pi-deficient condition. The Pi concentration of (A) leaf and (B) root. The expression of (C-D) *BnaA01.PAP17*, (E-F) *BnaA05.PAP17*, (G-H) *BnaC01.PAP17* and (I-J) *BnaC05.PAP17* in leaf and root. Seeds were germinated for six days and then grown in a Pi-sufficient (500 μM KH_2PO_4) nutrient solution for four days, and the seedlings were transferred to a solution without Pi for ten days, followed by two days recovery (R) in Pi-sufficient nutrient solution. The data are the means of four replicates with standard errors

Fig. 7 GUS staining of $Pro_{BnaA01.PAP17}$*::GUS* transgenic plants. GUS staining of (A) shoot and (B) root under +P and -P conditions, bar = 2 cm. GUS staining of primary root tip under (C) +P and (D) -P conditions, bar = 2 mm. Seeds were germinated for six days, and the seedlings were transferred to a Pi-sufficient (+P, 500 μM KH_2PO_4) nutrient solutions for four days, and then transferred to Pi-sufficient or Pi-deficient (-P, 0 μM KH_2PO_4) nutrient solutions for 15 days

Fig. 8 The difference in root-secreted APases activity and expression of *BnaPAP17s* among different *B. napus* accessions. (A) Root-secreted APases activity. (B-E) The expression of *BnaA01.PAP17* (B), *BnaA05.PAP17* (C), *BnaC01.PAP17* (D) and *BnaC05.PAP17* (E) in different *B. napus* accession roots. Seeds were germinated for six days and then transferred to Pi-sufficient (+P, 500 μM KH_2PO_4) or Pi-

deficient (-P, 0 μM KH_2PO_4) nutrient solution for five days. The data are the means of four replicates with standard errors. Significant difference based on Duncan's post-hoc analysis at $P < 0.05$

Fig. 9 Effects of overexpression of *BnaPAP17s* in *B. napus* on root-secreted APases activity and total P content. (A) The expression of *BnaPAP17s*. (B) The root-secreted APases activity, in *situ* staining for the root-associated APases activity, the yellow colour indicates the enzyme activity in roots. (C) The quantification root-secreted APases activity. (D) The total P content in shoots. The data are the means of four replicates with standard errors. Student's *t*-test was used for comparisons between two lines (**P* <0.05, ***P* <0.01, ****P* <0.001). +P, 500 μM KH_2PO_4; -P, 0 μM KH_2PO_4; ATP, 100 ATP

Supplementary data

Fig. S1 Frequency distribution of root-secreted APases activity in 350 accessions of *B. napus* under (A) Pi-sufficient (+P) and (B) -deficient (-P) conditions. (C) The difference in the root-secreted APases activity of the *B. napus* panel between +P and -P conditions. +P, 500 μM KH_2PO_4; -P, 0 μM KH_2PO_4

Fig. S2 Genome-wide association study for root-secreted APases activity of *B. napus* association panel under Pi-sufficient condition. The Manhattan and QQ plot by (A) GLM and (B) MLM. The horizontal dashed line represents the significance threshold with $-\log_{10}(P) = 5.77$ (red) and $-\log10(P) = 5$ (blue)

Fig. S3 Homology and phylogenetic analysis of BnaPAPs family. (A-B) Deduced amino acid sequence alignment of BnaPAP17s with AtPAP17. (C) The phylogenetic tree of PAPs in some species. It was constructed with MEGA 7.0 by neighbour-joining method. Bn, *Brassica napus*; At, *Arabidopsis thaliana*; Gm, *Glycine max;* Pv, *Phaseolus vulgaris*; Sg, *Stylosanthes guianensis*; Nt, *Nicotiana tabacum*; Os, *Oryza sativa*; La, *Lupinus albus*; Sl, *Solanum lycopersicum*; Mt, *Medicago truncatula*

Fig. S4 Biomass of wild-type (WT) and of transgenic plants with overexpression BnaPAP17 in B. napus under three P treatments. (A) Shoot and (B) root dry weight. Student's t-test was used for comparisons between two lines (*P < 0.05). +P, 500 μM KH_2PO_4; -P, 0 μM KH_2PO_4; ATP, 100 μM ATP.

Table S1 SAP activity of 350 accessions of *B. napus* used in this study under under Pi-sufficient and Pi-deficient conditions. SAP, root-secreted APases; Pi-sufficient (+P), 500 μM KH_2PO_4; Pi-deficient (-P), 0 μM KH_2PO_4

Table S2 Significant SNP loci for SAP activity of *B. napus* by GLM

Table S3 Significant SNP loci for SAP activity of *B. napus* by MLM

Table S4 The expression level of the genes in the confidence intervals of ChrA01_19576615 and ChrC03_3531206 in *B. napus* roots under Pi-sufficient and Pi-deficient conditions. The seeds were germinated for six days and then transferred to Pi-sufficient (+P, 500 μM KH_2PO_4) or Pi-deficient (-P, 0 μM KH_2PO_4) nutrient solution for five days

Table S5 Association analysis of BnaA01.PAP17 with root-secreted APases activity in *B. napus*

Table S6 Primers used in this study

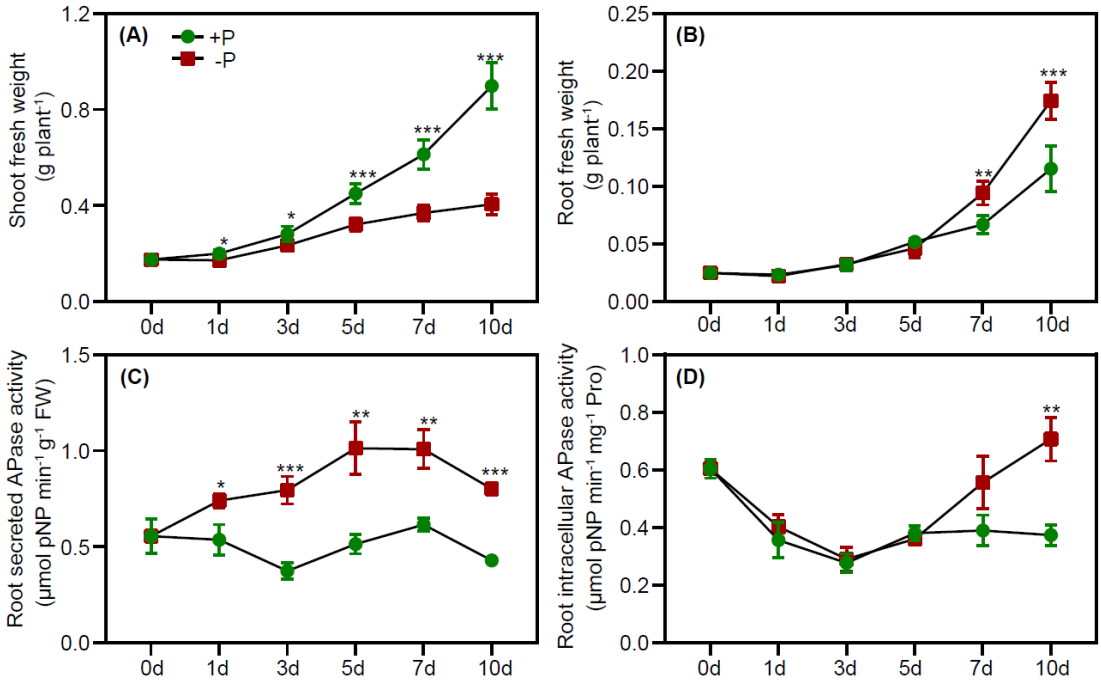

Fig. 1 Dynamic changes in shoot and root fresh weight, root-secreted and -intracellular APase activity in *B. napus*. (A) shoot and (B) root fresh weight. (C) Root-secreted APase activity and (D) root-intracellular APase activity. Seeds of 'Y127' were germinated for six days and then transferred to Pi-sufficient (+P, 500 μM KH_2PO_4) or -deficient (-P, 0 μM KH_2PO_4) nutrient solution for ten days. The data represent the means of six replicates for root and shoot fresh weight, and three replicates for root-secreted and -intracellular APase activity, along with their corresponding standard errors. Asterisks indicate significant differences between the -P and +P treatments by according to Student's *t*-test: **P* < 0.05; ***P* < 0.01; ****P* < 0.001.

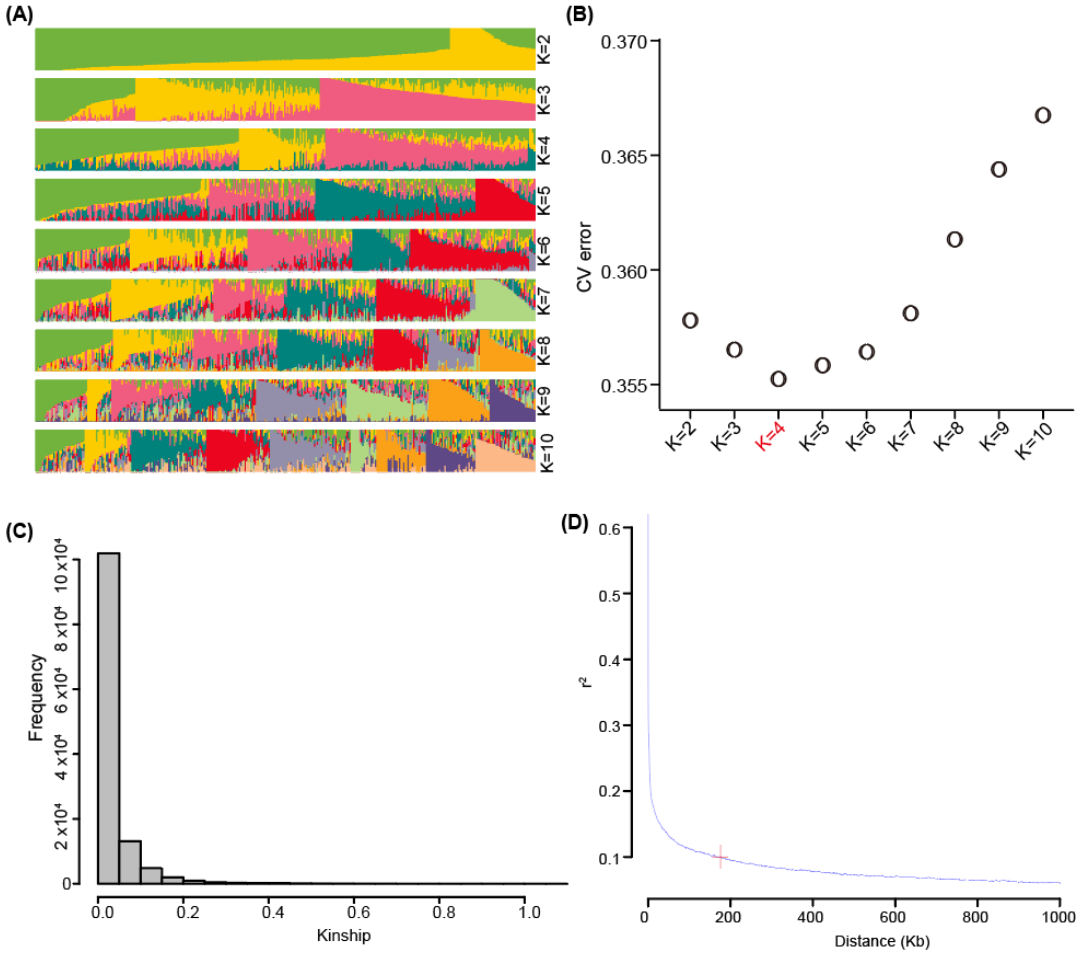

Fig. 2 The population structure, relative kinship and LD decay of the *B. napus* association panel. (A) The population structure plot. (B) The cross-validation error value. (C) The pairwise relationship of the *B. napus* association panel. (D) The LD decay plot, squared correlations of allele frequencies (r^2) at 0.1, LD decay distance of this natural population was 179 Kb.

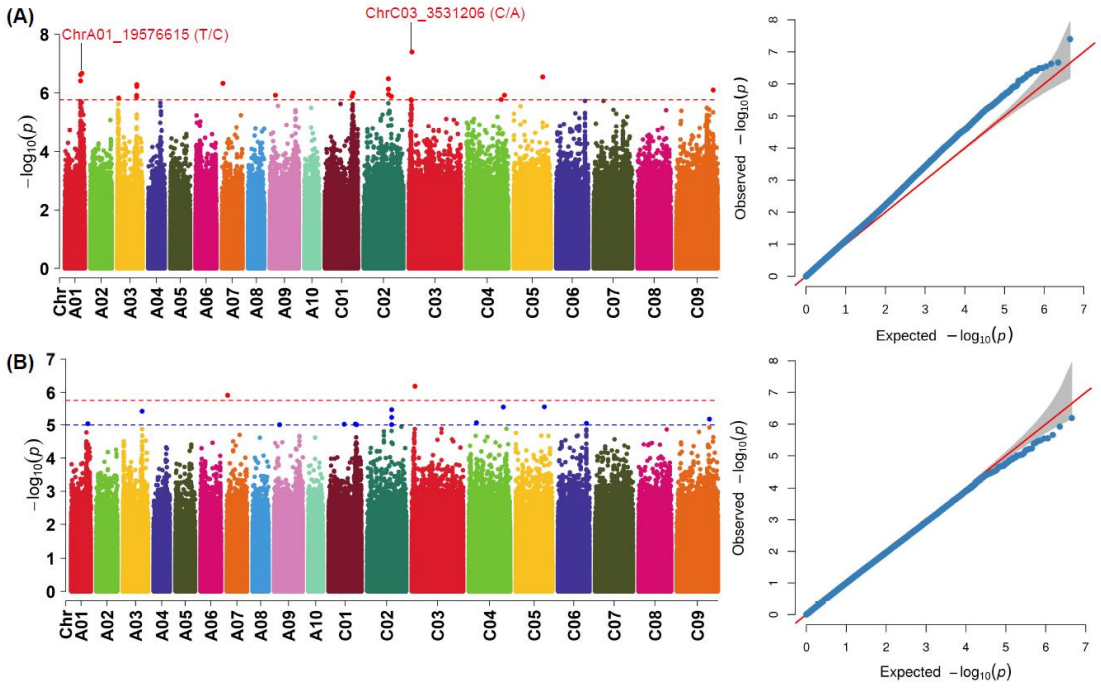

Fig. 3 Genome-wide association study for root-secreted APase activity of *B. napus* association panel under Pi-deficient condition. The Manhattan and QQ plot by (A) GLM and (B) MLM. The horizontal dashed line represents the significance threshold with -$\log_{10}(P)$ = 5.77 (red) and -$\log_{10}(P)$ = 5 (blue).

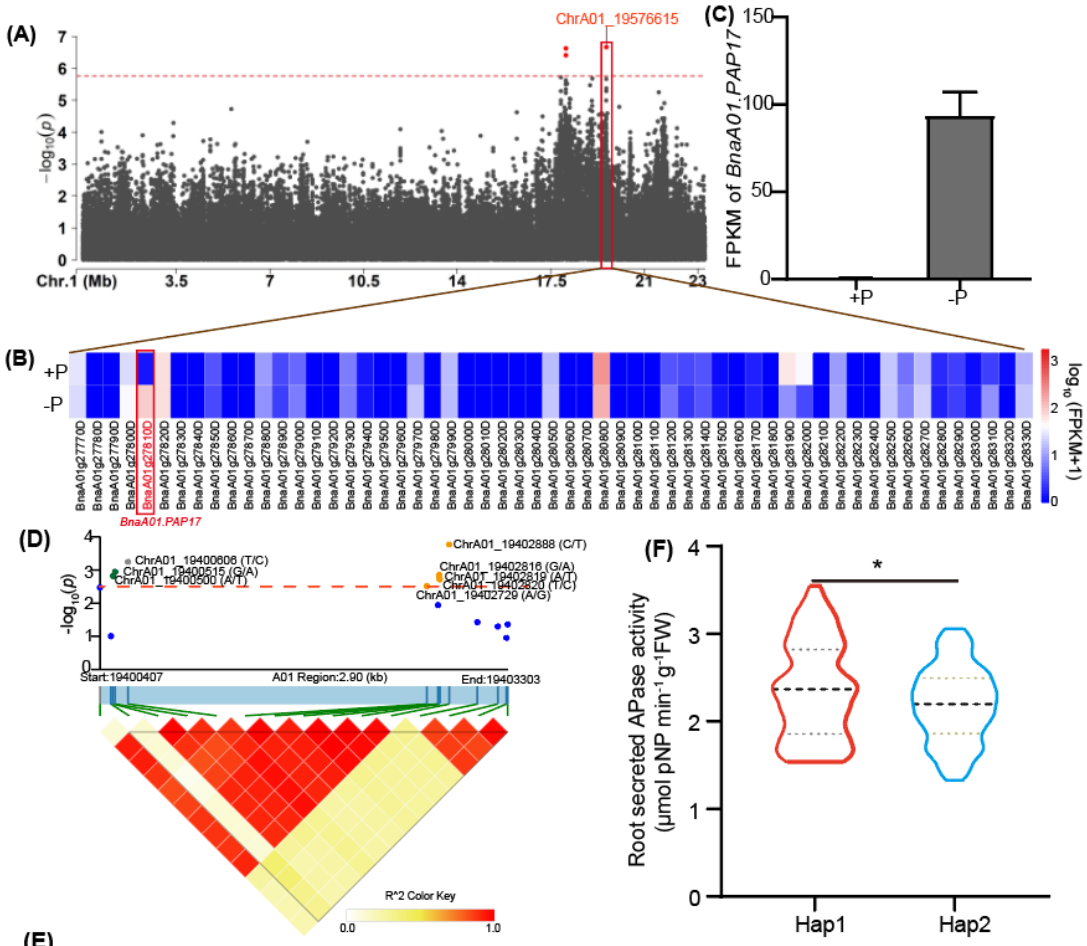

(E)

Position	19400500	19400515	19400606	19402729	19402816	19402819	19402820	19402888
Hap1(80)	T	A	C	G	A	T	C	T
Hap2(95)	A	G	T	A	G	A	T	C

Fig. 4 The significant SNPs associated with root-secreted APase activity on chromosome A01 and haplotype types of *BnaA01.PAP17* in the *B. napus* association panel. (A) The significant SNP locus on chromosome A01. (B) The expression level of the genes in the confidence interval of ChrA01_19576615 under Pi -sufficient (+P, 500 μM KH_2PO_4) and -deficient (-P, 0 μM KH_2PO_4) conditions. (C) The expression level of *BnaA01.PAP17*. (D) Candidate gene association analysis of *BnaA01.PAP17* with root-secreted APase activity, and the significant SNPs were located in exon (green), intron (grey) and yellow (promoter). (E) The haplotype types of *BnaA01.PAP17*. (F) The difference of root-secreted APase activity between Hap1 and Hap2, Student's *t*-test was used for comparisons between two haplotypes of *B. napus* ($*P < 0.05$).

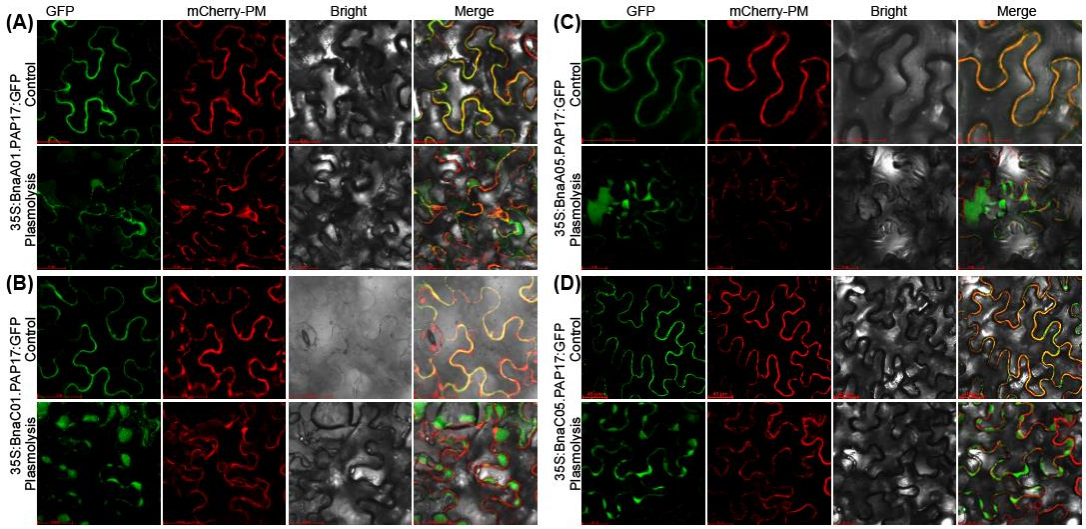

764

765 **Fig. 5 Subcellular localization of BnaPAP17s family.** GFP protein of (A) BnaA01.PAP17, (B) BnaC01.PAP17, (C) BnaA05.PAP17 and (D) BnaC05.PAP17 before or after plasmolyzing.

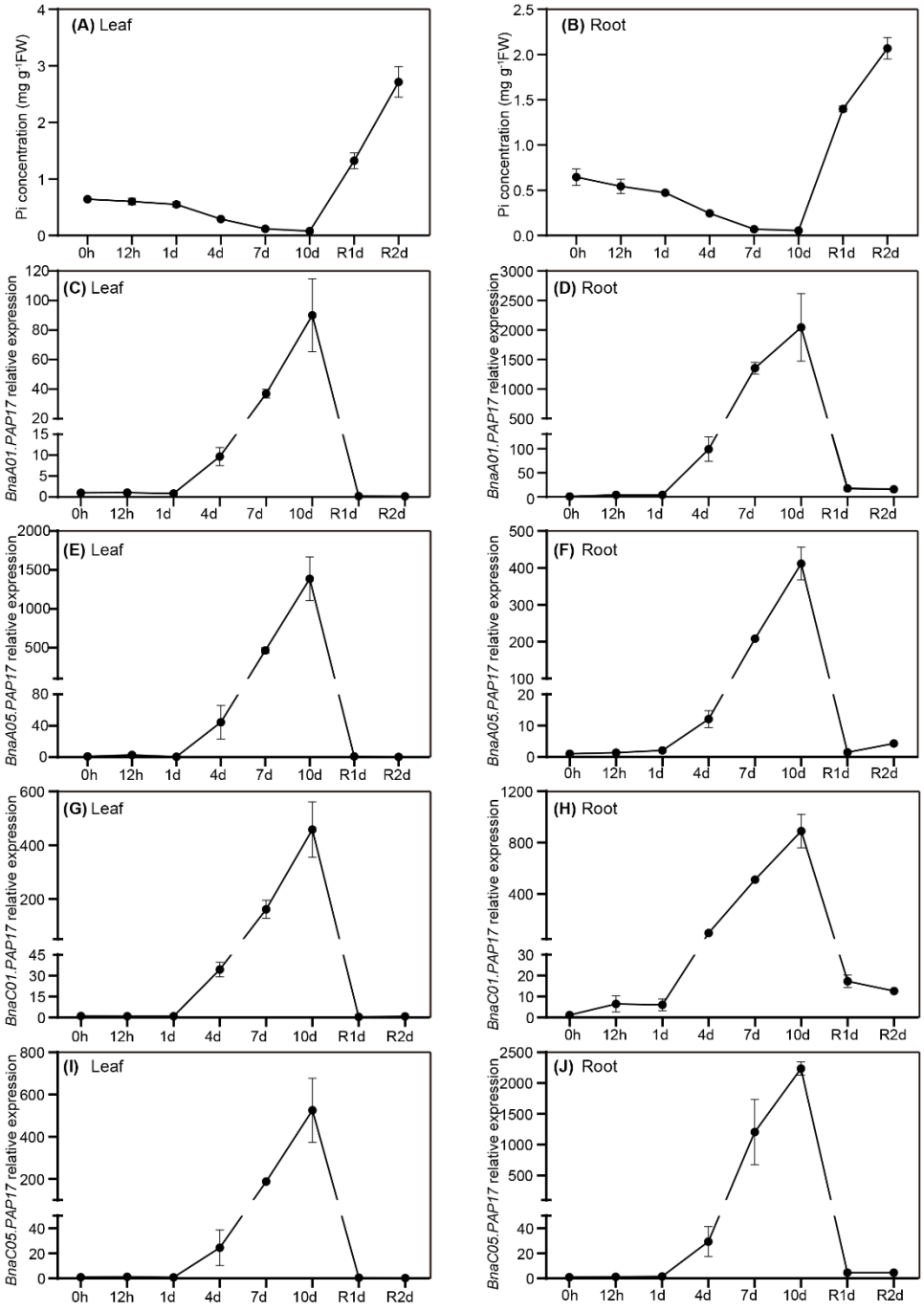

766

767

Fig. 6 Dynamic changes of Pi concentration and expression of *BnaPAP17s* in root and leaf under Pi-deficient condition. The Pi concentration of (A) leaf and (B) root. The expression of (C-D) *BnaA01.PAP17*, (E-F) *BnaA05.PAP17*, (G-H) *BnaC01.PAP17* and (I-J) *BnaC05.PAP17* in leaf and root. Seeds were germinated for six days and then grown in a Pi-sufficient (500 μM KH_2PO_4) nutrient solution for four days, and the seedlings were transferred to a solution without Pi for ten days, followed by two days recovery (R) in Pi-sufficient nutrient solution. The data are the means of four replicates with standard errors.

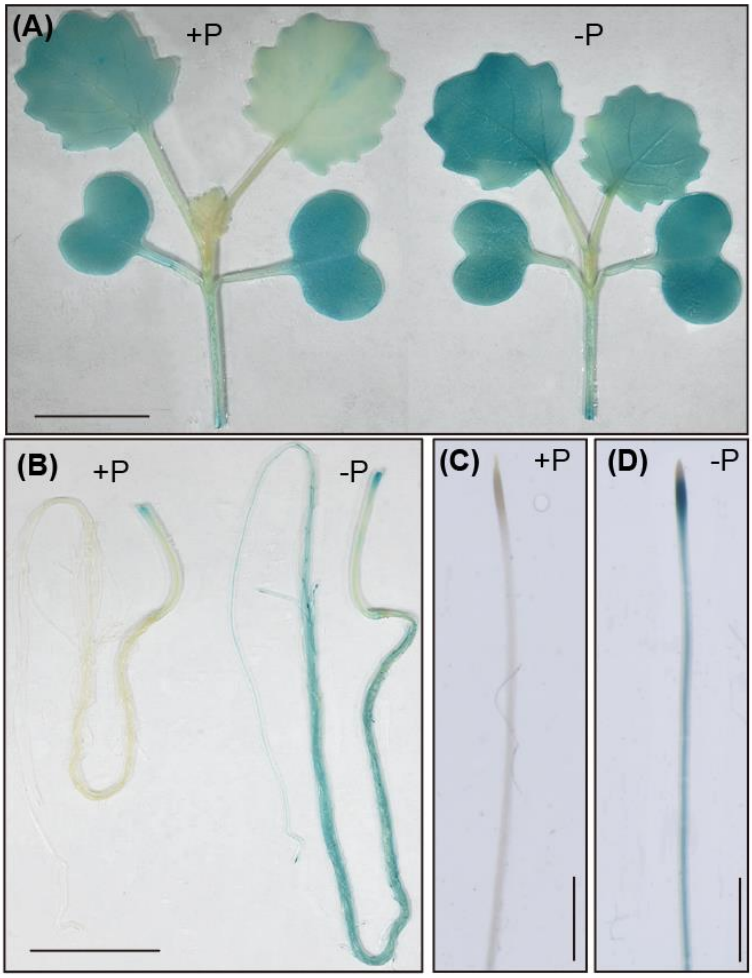

768
769

Fig. 7 GUS staining of *Pro*$_{BnaA01.PAP17}$*::GUS* transgenic plants. GUS staining of (A) shoot and (B) root under +P and -P conditions, bar = 2 cm. GUS staining of primary root tip under (C) +P and (D) -P conditions, bar = 2 mm. Seeds were germinated for six days, and the seedlings were transferred to a Pi-sufficient (+P, 500 μM KH_2PO_4) nutrient solutions for four days, and then transferred to Pi-sufficient or Pi-deficient (-P, 0 μM KH_2PO_4) nutrient solutions for 15 days.

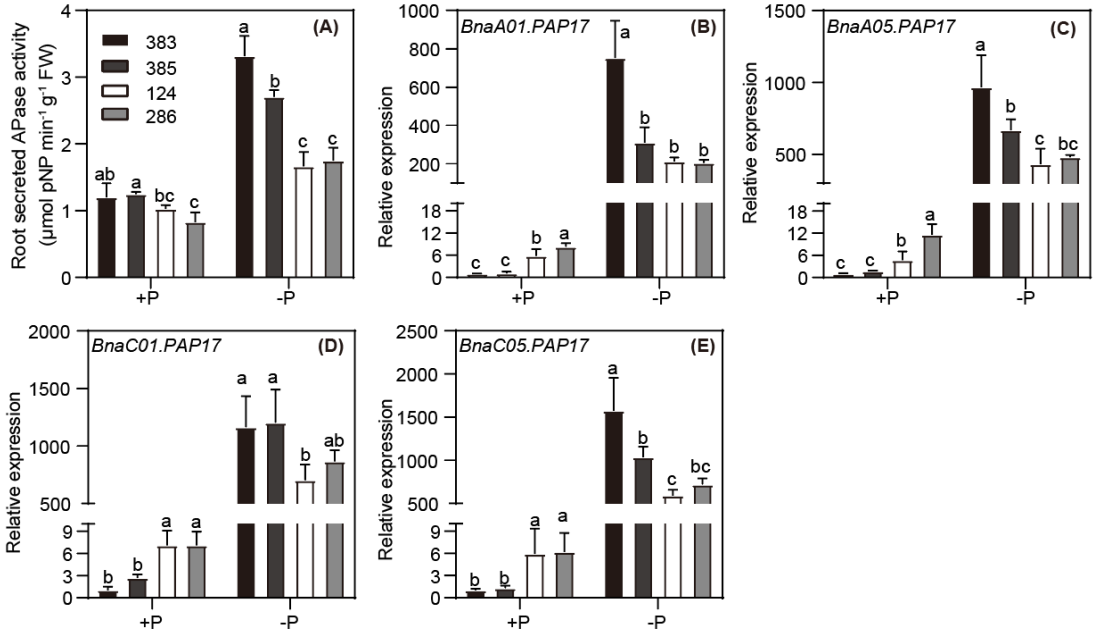

Fig. 8 The difference in root-secreted APase activity and expression of *BnaPAP17s* among different *B. napus* accessions. (A) Root-secreted APase activity. (B-E) The expression of *BnaA01.PAP17* (B), *BnaA05.PAP17* (C), *BnaC01.PAP17* (D) and *BnaC05.PAP17* (E) in different *B. napus* accession roots. Seeds were germinated for six days and then transferred to Pi-sufficient (+P, 500 μM KH_2PO_4) or Pi-deficient (-P, 0 μM KH_2PO_4) nutrient solution for five days. The data are the means of four replicates with standard errors. Significant difference based on Duncan's post-hoc analysis at $P < 0.05$.

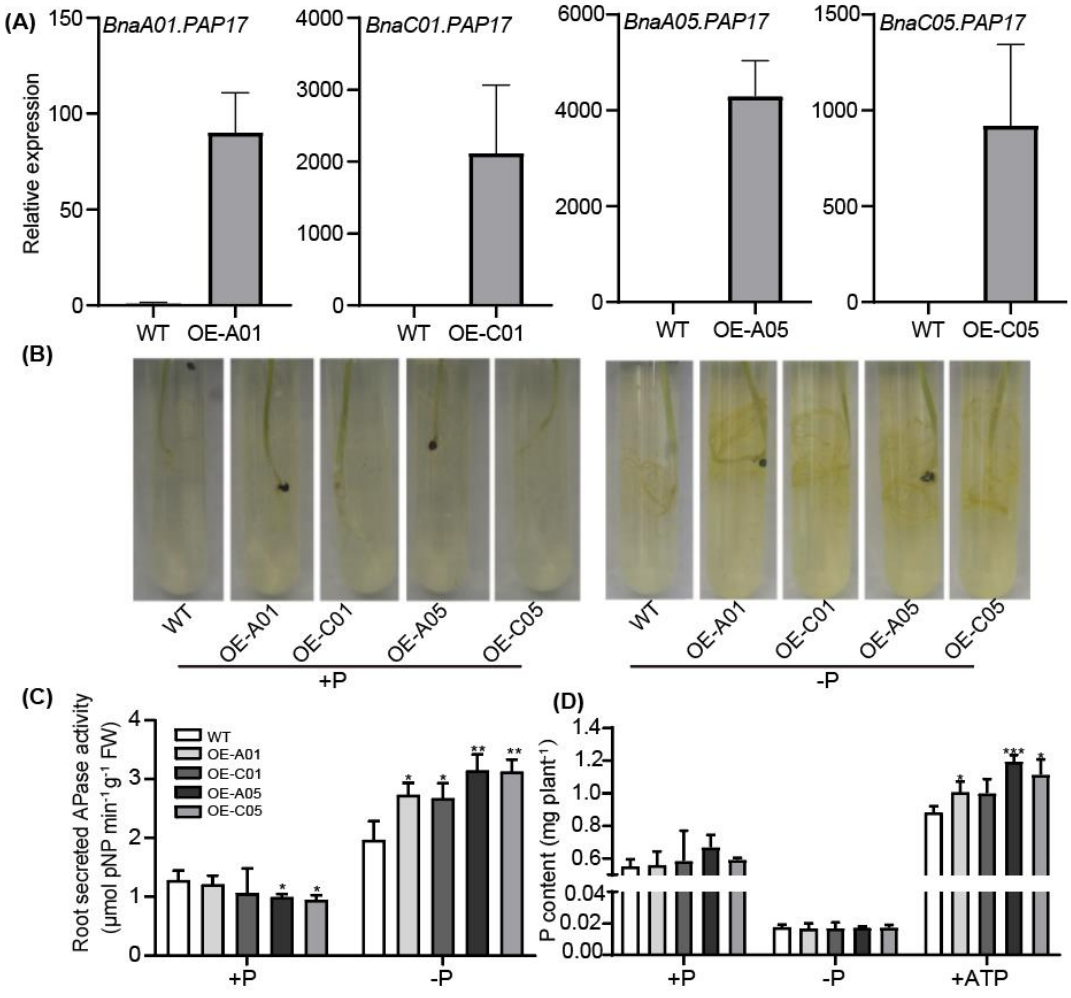

774

775 **Fig. 9 Effects of overexpression of *BnaPAP17s* in *B. napus* on root-secreted APase activity and total P content.** (A) The expression of *BnaPAP17s*. (B) The root-secreted APase activity, in *situ* staining for the root-associated APase activity, the yellow colour indicates the enzyme activity in roots. (C) The quantification root-secreted APase activity. (D) The total P content in shoots. The data are the means of four replicates with standard errors. Student's *t*-test was used for comparisons between two lines (**P* <0.05, ***P* <0.01, ****P* <0.001). +P, 500 μM KH_2PO_4; -P, 0 μM KH_2PO_4; ATP, 100 ATP.